VDMA
Fluid Power Association

22nd ISC

International Sealing Conference

Stuttgart, Germany
October 01 - 02, 2024

Sealing Technology –
Challenges accepted!

IMA
UNI STUTTGART

ISBN 978-3-8163-0768-6

Fachverband Fluidtechnik im VDMA e. V. Lyoner Str. 18
50628 Frankfurt am Main
Germany

Phone +49 69 6603-1513
E-Mail maximilian.baxmann@vdma.org
Internet www.vdma.org/fluid

Simulative Prediction of Leakage for Seat Valves and Bio-Hybrid Fuels

Marius Hofmeister, Felix Fischer, Lukas Boden, Katharina Schmitz

Seat valves play a critical role in various technical applications, such as automotive injectors. Here, predicting leakage is vital, as it can lead to poor combustion behaviour or complete system failure. To address this, a simulation model originally designed for predicting leakage of air in ball seat valves was adapted for the use with bio-hybrid fuels. Since many bio-hybrid fuels differ significantly in their fluid-mechanical properties from conventional fuels and gases like air, the simulation model cannot be used for these liquids without any adjustments. For this reason, additional experiments and simulations have been conducted for various bio-hybrid fuels. The corresponding results are compared and discussed in this study.

1 Introduction

Bio-hybrid fuels are produced based on renewable energy and non-fossil carbon sources. This way a closed carbon loop and CO2 neutral combustion is feasible. Therefore, bio-hybrid fuels are a promising alternative to other green energy carriers such as electric batteries and hydrogen. Within the excellence cluster “The fuel science center”, bio-hybrid fuels are investigated at a holistic level, with the aim of developing methods that can predict the properties of a fuel based solely on its molecular structure. This includes the prediction of combustion related properties like ignition delay, spray propagation and soot formation. Ultimately, these methods can be used to perfectly design a fuel to meet specific technical, economic, and ecological boundary conditions.

By using bio-hybrid fuels as drop-in fuels, existing vehicles and an extensive network of refineries and filling stations can be used, which is a further advantage over other alternative energy sources. To benefit from the mentioned advantages and to ensure safe operation, the compatibility with automotive components is a mandatory prerequisite. However, previous investigation revealed intolerable rates of swelling of elastomer sealing materials, bad lubrication and deviating fluid mechanical properties affecting spray propagation [1–7].

For safe operation especially the functionality of the injection system is of great importance, since unwanted leakage leads to poor combustion affecting engine efficiency and soot formation. In the worst case, leakage can result in damage to components or failure of the entire system. Since many bio-hybrid fuels differ significantly from conventional fuels in terms of their fluid-mechanical properties, it is necessary to check whether conventional injection systems can be used for these fuels or how they need to be modified. To address this, a simulation model originally designed for predicting leakage of air and hydrogen in metallic ball seat valves was adapted for the use with bio-hybrid fuels [8–14]. The aim of this study is to investigate the extent to which the deviating properties of bio-hybrid fuels influence poppet valves.

In the first part of this contribution the used simulation model is described.

Subsequently, the experimental setup for the validation of the simulation model is presented. Here, particular attention is paid to the measurement problems arising from the high vapor pressures of the liquids under investigation. Furthermore, the measurement methods for the determination of the fluid mechanical properties and the surface parameters needed for the simulation model are described. Afterward, the results obtained by means of the simulation model and the experimental results are discussed.

2 Simulation model

The simulation model used in this work is based on the contact mechanics model developed by Persson [15, 16] and a leakage model based on the Hagen–Poiseuille equation. The simulation method has been described comprehensively in previous works [10, 14]. This method can be separated into two distinct steps: a macroscopic simulation and a microscopic simulation. A schematic diagram of the simulation model can be seen in Figure 1. The constituent parts of the simulation are further described in the following subsections.

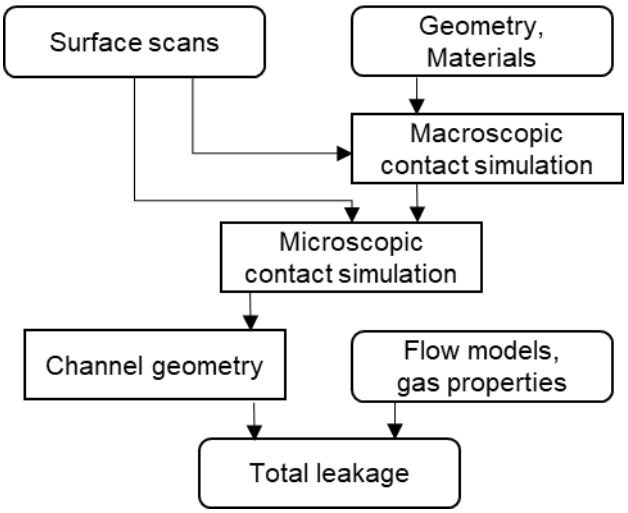

Figure 1 Scheme of the leakage simulation model

2.1 Macroscopic model

The macroscopic simulation model aims to calculate the contact pressure distribution at the sealing surface between the ball and the conical seat. The contact pressure distribution is calculated using an analytical description of the geometry of the ball and the seat at the contact area as well as the elastic material properties of both bodies.

It is important to incorporate the effects of surface roughness into this calculation. The nonzero roughness of all physical bodies leads to a smoothening of the calculated contact pressure distribution; it increases the contact area and reduces the maximal contact pressure. These effects can be included in analytical or numerical models like the finite element method (FEM) by calculating a relation between the distance of the surfaces and the contact pressure; this relation is called the contact–pressure relation.

There are multiple methods to calculate the contact–pressure relation; the most well-known being the Greenwood–Williamson method. This work uses the contact mechanics model developed by Persson two decades ago [16]. The Persson method is based on the spectral decomposition of the rough surfaces and can thus incorporate roughness of multiple length scales. This theory is also fit to describe the effects of the plastic deformation of the surface asperities leading to an increased leak-tightness compared to the purely elastic case.

The calculated contact pressure distributions of the rough surfaces in contact are in the next step used as input parameters of the microscopic simulation model.

2.2 Microscopic model

The microscopic model aims to predict the geometry of the microscopic slit (or more accurately the geometry of the systems of microscopic channels through the apparent contact area) causing the leakage through the valve, as well as calculating the resulting leakage.

The length of the leakage slit can be estimated by defining a contact width based on the contact pressure distribution determined in the previous simulation step. Meanwhile, the height of the channels at the determined contact pressure can be calculated by using a method developed by Persson based on his previously mentioned method [15]. This theory predicts the height of the microscopic net of channels using a percolation-based method. The percolation theory is a mathematical theory predicting the fraction of real contact area and contactless area, at which a free path is formed through a 2D porous medium, in this case, the contact area. The width and length of this critical path, as well as the macroscopic circumference of the contact area, are used to describe the geometry of the leakage slit.

Finally, the leakage through this microscopic slit is calculated using the Hagen–Poiseuille equation for the flow of viscous liquids through a thin rectangular slit.

3 Experimental setup

In the following the experimental setup used in this study is presented. This includes a test rig for the validation of the simulation results, measurements methods for the determination of the fluid mechanical properties needed for the execution of the simulation model, and the optical measurement methods for the evaluation of the surface parameters of the ball seat valve.

3.1 Leakage test rig

For the validation of the simulation the test setup shown in **Figure 2** was build up. The test rig mainly consists of a ball placed on a metallic seat. Due to a piston supplied by pneumatic pressure $p_{\mathrm{pneumatic}}$, the contact force between seat and ball is adjusted. At the inlet the test rig housing is connected to the pressurized sample liquid. From there the sample liquid flows through the sealing seat and the outlet. When leaving the outlet drops form, which are collected in a measuring cylinder. For the determination of the flow rate at the outlet of the test rig, two different methods are used in parallel. The first method is counting the number of droplets passing through the outlet. The determination of the droplet volume will be explained in more detail later. The second approach is measuring the volume flow directly with a measuring cylinder. Additionally, the flow rate is determined with help of a scale. The first method is suitable for low leakage rates, while the second method can be used for high leakage. Depending on the expected flow rate, three different measurement cylinders can be placed into the tube shown in Figure 2. The nominal and actual volume as well as the resolution and the standard deviation indicated by the manufacturer are listed in **Table 1** for each measurement cylinder.

Table 1: Volume and measuring resolution of the used measurement cylinders

Measurement cylinder	Nominal volume	Mean volume	Measuring resolution
1	10 ml	10,01 ± 0,01 ml	0,1 ml
2	25 ml	24,90 ± 0,02 ml	0,5 ml
3	50 ml	50,09 ± 0,06 ml	1,0 ml

The Accuracy of the described measurement principle depends highly on a constant and time-independent droplet size. However, due to the high vapor pressure of some investigated fuel, an evaporation rate can be expected, which is high compared to the measured leakage flow and avoids precise evaluation of flow rate. For this reason, the described setup was adjusted for the use of low-boiling liquids. To avoid evaporation during the measurement process, an additional tube is mounted at the outlet of the test rig, which is sealed to the atmosphere (Figure 2). Inside of the tube a measuring cylinder is placed. Before each measurement series, the measuring cylinder is filled with corresponding sample liquid. Now the sample liquid starts to evaporate, whereupon the level in the measuring cylinder lowers. When the liquid level inside the measuring cylinder doesn't change anymore, the thermodynamic equilibrium is reached, and no more evaporation occurs during the actual measuring process.

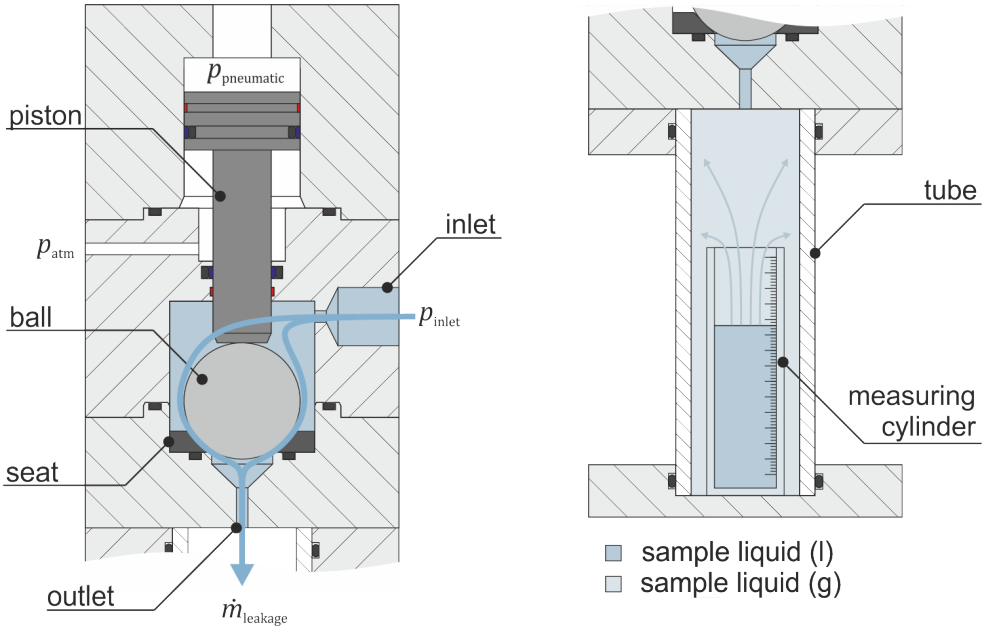

Figure 2 Test rig for the determination of leakage flow rate

Since leakage strongly depends on the viscosity and density and therefore on the liquid temperature, the temperature in the laboratory is measured for each test process. Afterwards, the measured temperature is used to calculate the fluid mechanical properties based on the measurement results presented in section 4.1. The corrected fluid mechanical properties are used as input parameters for the simulation model.

3.2 Determination of droplet volume

To measure the leakage for small flow rates precisely, the droplet volume for the different sample liquids must be estimated with sufficient accuracy. To check the plausibility of the measured droplet volume, the size of the droplets is also estimated by evaluating the surface and gravitational forces acting at the outlet (**Figure 3**).

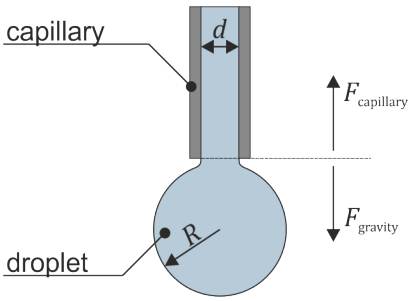

Figure 3 Equilibrium of forces at outlet capillary

The equilibrium of surface and gravitational forces is shown in equation (1). The capillary force $F_{\mathrm{capillary}}$ is the product of the liquid surface tension σ and the capillary diameter d_c multiplied by π. The gravitational force F_{gravity} acts against the capillary force and depends on the droplet volume V_{D} and the liquid density ρ.

$$\sum_{i=1}^{n} F_i = \underbrace{\sigma d_{\mathrm{c}} \pi}_{F_{\mathrm{capillary}}} - \underbrace{V_{\mathrm{D}} \rho \mathrm{g}}_{F_{\mathrm{gravity}}} \tag{1}$$

If both forces are in equilibrium, the droplet volume reaches its maximum and can be calculated with (2).

$$V_{\mathrm{D}} = \frac{\sigma d_{\mathrm{c}} \pi}{\rho \mathrm{g}} \tag{2}$$

In this study a capillary made of stainless steel with an inner diameter d_c of 0.6 mm and an outer diameter of 0.8 mm was used.

3.3 Determination of fluid mechanical properties

For the calculation of leakage and the estimation of droplet volume, the fluid mechanical properties viscosity, density and surface tension are necessary. In the following the measurement methods used for the determination of these values are presented.

Kinematic viscosity

The kinematic viscosity of the different fuels is determined by means of an Ubbelohde viscometer according to DIN 55660 [17]. For tempering the sample liquid during the measurement, a temperature control unit with an accuracy of 0.01 K is used. At the beginning of the experiment, the Ubbelohde viscometer is filled with sample liquid and is placed into the temperature control unit. To ensure a constant temperature level of the liquid, the actual measurement starts 30 minutes after the viscometer were placed into the temperature control unit. An overall number of 7 sub measurements is conducted for each temperature step, whereby the first two measurements are meant to flush the capillary of the viscometer and are not considered for the evaluation of viscosity. The mean value is calculated from the remaining 5 measurements. For all measurements, care was taken to ensure that the measurement time was not less than 100 s.

Density

The liquid density is measured by help of the Archimedean principle [2, 18]. In total 10 sub measurements are carried out from which the mean value is calculated. For the temperature control of the liquid the same system is used as for the determination of kinematic viscosity.

Surface tension

The surface tension of the sample liquids was determined by the du Noüy ring method in accordance with DIN EN 14370 [19]. The used tension scale has a measurement resolution of 0.1 mg. In total 10 measurements are conducted for each fuel and each temperature step. The temperature of the sample liquid is controlled by a temperature control unit with a temperature accuracy of 0.02 K.

4 Results and discussion

In the following the results obtained in this study will be shown. First, the results for the fluid mechanical properties viscosity, density and surface tension are shown. Afterwards, the measured and the simulated leakage rates are presented.

4.1 Fluid mechanical properties

In **Figure 4** the results for the viscosity measurements described in 3.3 are shown for EN 590, Ethanol and Acetone for a temperature range between 10 and 30 °C. Overall a low standard deviation less than 0.5 % could be achieved for each liquid and temperature step. The highest values for viscosity are obtained for EN 590 with 3.898 mm²/s at 20 °C. The viscosity of ethanol and acetone is significantly lower than for diesel EN 590 (1.5 mm²/s, 0.317 mm²/s).

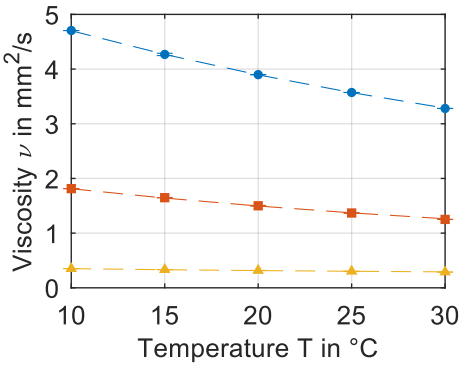

Liquid	A	B	C
EN 590	0.123	0.079	0.183
Ethanol	670.2	480.5	33.11
Acetone	173.7	143.4	40.64

Figure 4 Results for kinematic viscosity and corresponding Arrhenius coefficients

To correct the viscosity values for the simulation model, based on the measurement data and the Arrhenius equation visible in (3) a regression analysis was performed.

$$\nu(T) = A \cdot \exp\left(\frac{B}{C+T}\right) \tag{3}$$

With help of (3) and the calculated Arrhenius coefficients listed in Figure 4 the viscosity can be calculated for varying liquid temperatures during the leakage experiment.

The results for the density measurements and the coefficients of the linear regression analysis are shown in **Figure 5**. The standard deviation for each measuring point is less than 1 %.

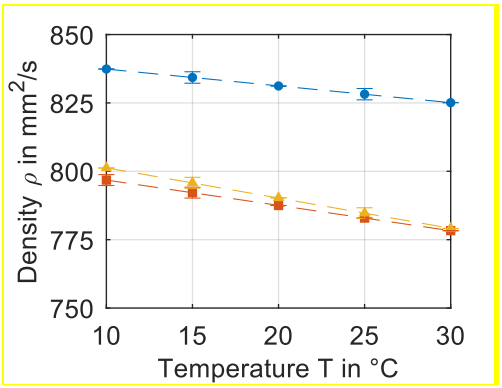

Liquid	A	B
EN 590	843.5	-0.614
Ethanol	806.1	-0.926
Acetone	812.3	-1.106

Figure 5 Results for density and corresponding linear coefficients

In **Figure 6** Results for surface tension and corresponding linear coefficients the results for the surface tension measurements conducted with the du Noüy ring method are shown. Just as with the density results, a linear regression analysis was performed. The corresponding coefficients of the analysis are shown in Figure 6.

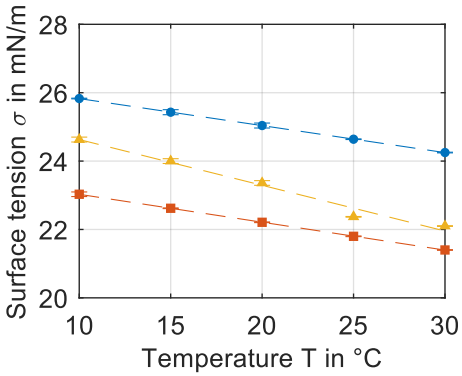

Liquid	A	B
EN 590	26.62	-0.079
Ethanol	23.84	-0.082
Acetone	25.97	-0.134

Figure 6 Results for surface tension and corresponding linear coefficients

4.2 Droplet size

Depending on the fluid mechanical properties determined in 4.1 the droplet size was calculated according to the simplified approach described in (2). The results for temperatures in a range between 10 and 30 °C are shown in **Figure 7**.

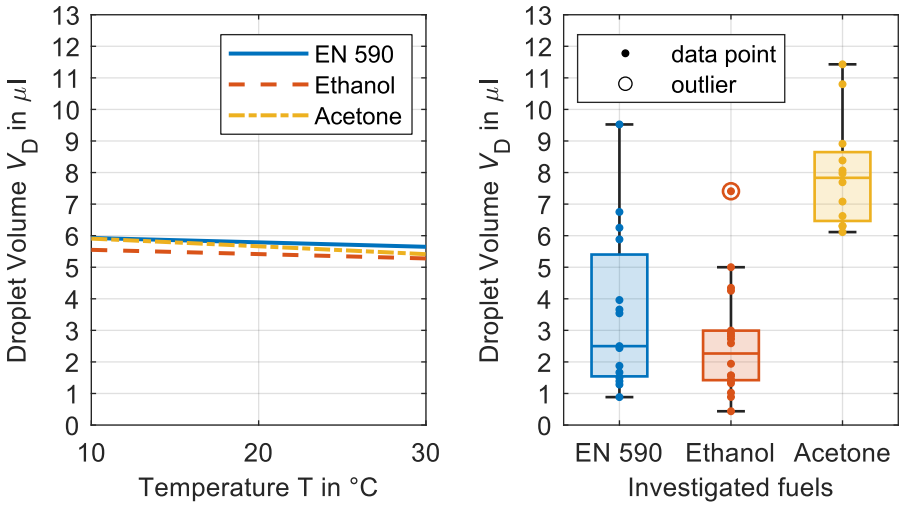

Figure 7 Estimated droplet volume V_D and measured droplet size deviation

Due to the high surface tension the droplet volume of EN 590 is the highest in the considered temperature range. The values for Ethanol and Acetone are slightly lower but in the same order of magnitude.

The results show that the droplet volume in the relevant temperature range depends insignificantly on the temperature. The target temperature during the leakage tests is 20 °C. Assuming a maximum temperature deviation of 2 °C during or between individual experiments, the maximum deviation of the drop volume is only 0.48 % for EN 590. For ethanol and acetone, the maximum deviation is 0.50 and 0.87 %.

The estimated droplet volume was also used to check the plausibility of the measured droplet sizes. On the right-hand side in Figure 7 one can see the results for the droplet volume obtained with the methods described in 3.2. As can be seen the results are in the same order of magnitude for the calculated and measured values. However, for each fuel a high deviation in droplet size is obtained. In case of EN 590 and Ethanol the measured mean value is below the calculated drop size. For Acetone the simplified underestimates the measured mean value.

4.3 Leakage

The leakage measurements described in 3.1 were carried out for two different seats differing in surface properties. In **Figure 8** the results for the flow rate measurements are shown for the investigated liquids and seat 1. For all fuels and seats a pneumatic

piston pressure and a fluid pressure of 3 bar was applied. Although all measurements were carried out under similar boundary conditions, there are large deviations within the individual measurement series. This is most evident for the diesel measurement. Here, the averaged flow rate for measurement 2 is 27 µl/s and therefore one order of magnitude higher than for measurement 1 and 3 (2.3 µl /s and 1.8 µl/s).

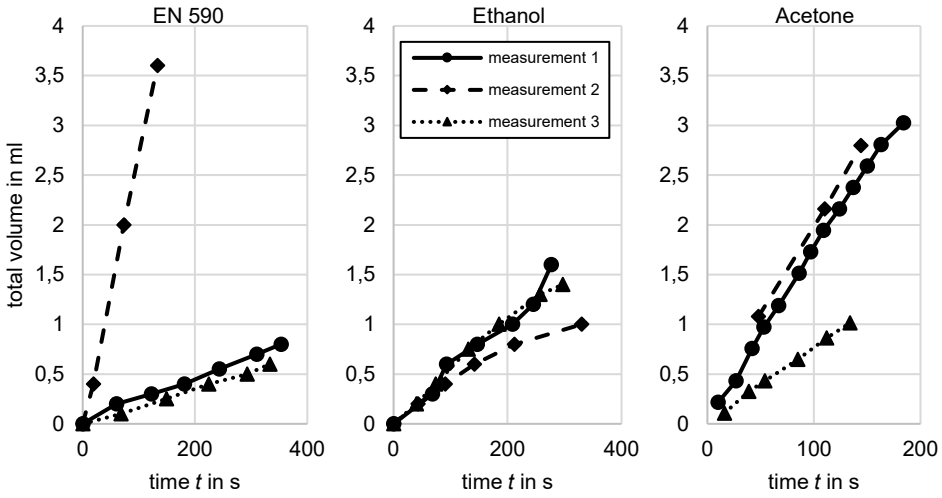

Figure 8 Flowrate measurements for seat 1

For ethanol and acetone, the results are more reproducible than for EN 590, although they still differ greatly from each other. Furthermore, the results show that the volume flow decreases after a certain time. This phenomenon can be seen most clearly for ethanol and the sub measurements 2 and 3. While the average flow rate at the beginning of the measurement between the first two increments is 4.65 µl/s (measurement 2) and 5.00 µl/s, it decreases significantly over time. At the end of each measurement series, the flow rate for measurement 2 is 1.69 µl/s and for measurement 3 2.50 µl/s. Here it was assumed that during the measurement, particles increasingly accumulate in the contact between the ball and the seat, which gradually close the gap and reduce the flow rate.

Similar behavior is already known from measurements with distilled water. Here it was assumed that during the measurement, particles increasingly accumulate in the contact between the ball and the seat, which gradually close the gap and reduce the flow rate. For measurements performed with nitrogen as sample fluid, this behavior could not be observed. For this reason, it is assumed that particles are also responsible for the phenomena shown in this case [12, 13].

The averaged results for the measured leakage flow rate and for the simulated flow rate are listed in **Table 2**. As already indicated in Figure 8, the repeatability of the leakage measurements is poor, which is reflected in a high standard deviation for all

seats and liquids examined. In the case of diesel and seat 2, the standard deviation is even greater than the calculated mean value.

It can also be seen that the measured leakage is very high compared to the simulated values. For most measured values are one order of magnitude higher than calculated.

Table 2: Measured and simulated leakage flow rate for different seats

		Seat 1		Seat 2	
		S_Q = 2.53	γ = 0.75	S_Q = 1.9	γ = 0.35
		Leakage in µl/s		Leakage in µl/s	
Sample liquid	Viscosity in mm²/s	measured	simulated	measured	simulated
Acetone	0.317	66 ± 17	5.1	17 ± 6	2.6
EN 590	3.898	12 ± 6	0.47	10 ± 12	0.25
Ethanol	1.500	55 ± 20	1.3	5.1 ± 1.4	

The investigated seats differ from each other regarding their surface properties indicated by the mean squared roughness value S_Q and the Peklenik number γ. In this context an infinite Peklenik number corresponds to a surface with grooves in parallel to the flow direction. An Peklenik number equal to zero is related to grooves aligned orthogonally to the direction of flow. Consequently, the surface of seat 1 is rougher, and the surface peaks are more aligned in flow direction than for seat 2. Both factors promote leakage flow. This trend can be seen both in the measurement results and in the results of the simulation.

5 Summary and Conclusion

In this paper, a simulation model for the investigation of leakage in ball seat valves and corresponding methods for the experimental validation of the leakage flow were presented. A particular focus was placed on the challenges arising from the low viscosity and high vapor pressure of many bio-hybrid fuels.

Subsequently, the experimental results and the results of the simulation were presented. It was found that the results for leakage vary greatly. This is especially true for EN 590. A probable reason for the large deviations could be the contamination of the test liquids by particles.

It was also found that the simulation underestimates the leakage by an order of magnitude, which can also be explained by particles that prevent the valve from closing completely.

Overall, the high standard deviations of the measurement results make a meaningful comparison with the simulation results difficult. For this reason, future investigations will focus on the improvement of reproducibility. This primarily involves the systematic investigation of the particle load of the test liquids used and a finer pre-filtering

of the liquids. The tests are then repeated using the filtered liquids with a defined particle load.

At the same time, the results also show that the qualitative trends like the influence of surface parameters and viscosity on the leakage can already be correctly captured by the simulation.

6 Acknowledgements

Funded by the Deutsche Forschungsgemeinschaft (DFG, German Research Foundation) under Germany´s Excellence Strategy – Exzellenzcluster 2186 „The Fuel Science Center".

7 Nomenclature

Variable	*Description*	*Unit*
A B C	Coefficients for regression analysis of fluid mechanical properties	
d_c	Capillary diameter	[mm]
$F_{\mathrm{capillary}}$	Capillary force	[N]
F_{gravity}	Gravitational force	[N]
g	Gravitational constant	[m/s²]
$\dot{m}_{\mathrm{leakage}}$	Leakage mass flow	[kg/s]
p_{atm}	Atmospheric pressure	[bar]
p_{inlet}	Inlet pressure	[bar]
$p_{\mathrm{pneumatic}}$	Pneumatic pressure	[bar]
R	Droplet radius	[mm]
S_Q	Mean square roughness	[µm]
T	Temperature	[°C]
V_{D}	Droplet volume	[ml]
γ	Peklenik number	[-]
σ	Surface tension	[mN/m]
ρ	Liquid density	[kg/m³]
ν	Kinematic viscosity	[mm²/s]

8 References

[1] HOFMEISTER, Marius; Boden, Lukas; Schmitz, Katharina: *Challenges in the Use of Bio-hybrid Fuels as Drop-in Fuel*. In: *ASME 2024 - 18th International Conference on Energy Sustainability* (2024)

[2] HOFMEISTER, Marius, et al.: Tribological properties of PTFE sealing materials with regard to bio-hybrid fuels. In: *Sealing technology - old school and cutting edge* : *International Sealing Conference : 21st ISC, Stuttgart, Germany, October 12-13, 2022*. Frankfurt am Main : Fachverband Fluidtechnik im VDMA e.V, 2022, S. 89–104

[3] HOFMEISTER, Marius, et al.: *Neue Herausforderungen an Dichtungswerkstoffe im Hinblick auf bio-hybride Kraftstoffe*. In: *Mobility 7* (2022), RWTH-2022-09721. URL https://publications.rwth-aachen.de/record/854697

[4] HOFMEISTER, Marius, et al.: Optimization of Bio-hybrid Fuel Blends regarding Material Compatibility with Elastomer Seals. In: *11th FSC* : *Fuel Science - From Production to Propulsion*, 2023

[5] VÖLKER, Simon, et al.: The drop-in potential of hydroformylated Fischer-Tropsch fuels from CO2. In: *11th FSC* : *Fuel Science - From Production to Propulsion*, 2023

[6] VÖLKER, Simon, et al.: Towards sustainable transport with hydroformylated Fischer-Tropsch fuels as drop-in fuels employing drop-in technology. In: *11th FSC* : *Fuel Science - From Production to Propulsion*, 2023

[7] GRÜTERING, Carolin; Honecker, C.: *Methyl ketones: a comprehensive study of the last biofuel* (2023)

[8] FISCHER, Felix J., et al.: Finite Element Analysis of the Hard-Hard Contact in Seat Valves. In: *Global Fluid Power Society PhD Symposium*.

[9] FISCHER, Felix J.; Bady, Dariush; Schmitz, Katharina: *Leakage of Metallic Ball Seat Valves with Anisotropic Surfaces*. In: *Chemical Engineering & Technology* 46 (2023), Nr. 1, S. 102–109

[10] FISCHER, Felix J.; Murrenhoff, Hubertus; Schmitz, Katharina: *Influence of normal force in metallic sealing*. In: *Engineering Reports* 3 (2021), Nr. 10

[11] PENG, Chao, et al.: *Comparative analysis of leakage calculations for metallic seals of ball-seat valves using the multi-asperity model and the magnification-based model*. In: *Tribology International* 163 (2021), S. 107130

[12] FISCHER, Felix J.; Peng, Chao; Schmitz, Katharina: Research on Leakage Characteristics of Metallic Seals Based on Soft/Hard Contact Theories. In: *10. International Conference on Fluid Power Hangzhou*.

[13] FISCHER, Felix J., et al.: *Geometry of Ball Seat Valves*. In: *International Journal of Fluid Power* (2021)

[14] FISCHER, Felix. J., et al.: *Fluid Leakage in Metallic Seals*. In: *Tribology Letters* 68 (2020), Nr. 4

[15] PERSSON, B. N. J.: *Fluid dynamics at the interface between contacting elastic solids with randomly rough surfaces*. In: *Journal of physics. Condensed matter : an Institute of Physics journal* 22 (2010), Nr. 26, S. 265004

[16] PERSSON, B. N. J.: *Theory of rubber friction and contact mechanics*. In: *The Journal of Chemical Physics* 115 (2001), Nr. 8, S. 3840–3861

[17] 1976. *DIN 55660:1976-02*

[18] GRÜTERING, Carolin, et al.: *Methyl ketones: a comprehensive study of a novel biofuel*. In: *Sustainable Energy & Fuels* 8 (2024), Nr. 9, S. 2059–2072

[19] 2004. *DIN EN 14370:2004-11*

9 Authors

RWTH Aachen - Institut für fluidtechnische Antriebe und Systeme (ifas),

Campus-Boulevard 30, 52074 Aachen, Germany:

Marius Hofmeister, M. Sc., ORCID 0000-0002-6672-5800,
marius.hofmeister@ifas.rwth-aachen.de

Felix Fischer, M. Sc., ORCID 0000-0003-2081-1823,
f.fischer@ifas.rwth-aachen.de

Lukas Boden, M. Sc., ORCID 0009-0003-1282-8032,
lukas.boden@ifas.rwth-aachen.de

Univ.-Prof. Dr.-Ing. Katharina Schmitz, ORCID 0000-0002-1454-8267,
katharina.schmitz@ifas.rwth-aachen.de

https://doi.org/10.61319/HTXAF9PX